

Morphological features of Co_3O_4 nanoparticles obtained by solution combustion method

A. Keneshbekova^{1*}, A. Imash^{1,2}, B. Kaidar¹, E. Yensep², A. Ilyanov²,
M. Artykbayeva¹, N. Prikhodko^{1,3}, G. Smagulova¹

¹Institute of Combustion Problems, 172 Bogenbay Batyr str., Almaty, Kazakhstan

²Al-Farabi Kazakh National University, 71 Al-Farabi ave, Almaty, Kazakhstan

³Gumarbek Daukeev Almaty University of Energy and Communications,
126/1 Baitursynuly str., Almaty, Kazakhstan

ABSTRACT

The global environmental crisis has made it imperative to enhance tools and techniques for monitoring and analyzing environmental parameters. Gas sensors, crucial for air quality assessment, continually undergo technological advancements to enhance accuracy and efficiency in detecting harmful substances. They play an essential role in ensuring safety in workplaces, urban areas, and industries, aiding pollution control efforts. Enhanced gas sensor performance hinges on careful selection and control of gas-sensitive materials and their structure. This involves optimizing gas-sensitive compounds, employing advanced materials, and developing technologies for sensitive and rapid substance detection. One promising compound for this purpose is Co_3O_4 oxide, synthesized efficiently using the solution combustion method. This method offers simplicity and allows for precise control over product structures and properties, enabling customization for specific requirements and ensuring high detection efficiency and accuracy. In this study, Co_3O_4 particles were synthesized from a mixture of cobalt nitrate and glycine with the addition of nitric acid using the solution combustion method. The influence of nitric acid addition and the fuel-to-oxidizer ratio on the morphological characteristics of the cobalt oxide was investigated. The results from SEM, TEM, XRD, and SAXS analyses confirmed that the addition of nitric acid and a fuel-rich mixture lead to nanoparticles with smaller diameter spread and more stable characteristics.

Keywords: metal oxide nanomaterials, Co_3O_4 nanoparticles, solution combustion method, exothermic redox reaction, gas sensors.

1. Introduction

Nowadays, gas sensors are attracting considerable attention from researchers due to the aggravated environmental problems. Gas sensors are of paramount significance in determining the type and concentration of pollutants in the air. There are different types of gas sensors such as semiconductor, photoionization, electrochemical, etc. [1].

Conductometric semiconducting metal oxide gas sensors, also, is one of the groups of gas sensors suitable for conducting gas measurements under atmospheric conditions. They have several advantages including flexibility in manufacturing, ease of use, low cost, and, most importantly, the ability to detect a wide range of gases [2].

An essential characteristic of conductometric semiconducting metal oxide gas sensors is the reversible interaction of gas with the material surface, which can be affected by the natural properties of the basic components, microstructure of the sensing layers, surface area, and external factors such as temperature and humidity [2-7]. The sensitivity of gas sensors plays an important role in their operation. However, there is currently no single and universal gas sensor for the detection of different gases. Therefore, various transition metal oxides like Fe_2O_3 [8], Cr_2O_3 [9], NiO [10], and non-transition metal oxides including pre-transition metals like ZnO [11], Al_2O_3 [12], SnO_2 [13], and so on are used in conductometric meters for the detection of combustible, oxidizing and reducing

**Ответственный автор*
E-mail: keneshbekova.a0204@gmail.com

gases. Inertness, structure stability, and the easiness of measuring the electrical conductivity, which depends on the electronic configuration, are the main parameters in the selection of oxides for gas sensors. Despite the wide range of oxides, transition metal oxides with d^0 and d^{10} electron configurations have a practical application in gas sensors. Such oxides include TiO_2 [14], WO_3 [15], and Co_3O_4 [16].

Co_3O_4 stands out among the others because it is a p-type oxide with the structure of spinel AB_2O_4 and a forbidden band energy of 1.6–2.2 eV [17]. Due to its structure, Co_3O_4 has high stability, specific capacitance (500–700 F/g [18]), electrical conductivity (charging capacity 900–1000 mAh/g [19]), large surface area (more than 90 m^2/g [18]) and pore volume (135.72–292.66 cm^3/g [19]). Authors [17-20] investigated gas sensors based on cobalt oxide and found that it has a high potential in gas detection.

In addition, cobalt oxide nanoparticles can be used in magnetic materials [21], ceramic pigmentation [22], as a catalyst [23], electrochromic devices [24], and rechargeable batteries [19]. Therefore, the synthesis of cobalt oxide powder with improved characteristics has attracted huge interest recently.

There are numerous methods for the synthesis of cobalt oxide. However, each of them has its own advantages and disadvantages, and the choice of the method depends on the area and purpose of the material application.

As can be seen from Table 1, despite the various methods for the synthesis of cobalt oxide, obtaining homogeneous nanoparticles remains a costly method because controlling the size, shape, and morphology of the product, as well as the valence of cobalt ions like Co^{3+} and Co^{2+} , is a labor-intensive process. Moreover, for extensive applications of Co_3O_4 , including in gas sensors, the oxide must have high stability and dispersion. Also, it is necessary to properly approach the issue of synthesis waste disposal, for example, in the synthesis of nanoparticles by co-precipitation, in general, besides metal oxide, many compounds are formed, which are difficult to utilize. Therefore, a more ecological method of synthesis of Co_3O_4 should be preferred.

Among a variety of methods for the synthesis of cobalt oxide, the solution combustion method is highlighted. It is based on the self-propagating combustion of a mixture of fuel and oxidizer in the liquid phase. Gradual heating of reagents dissolved in water leads to an exothermic redox reaction resulting in the formation of metal oxide [17, 30]. Compared to other methods, this method is characterized by simplicity, practicality, and rapidity.

Furthermore, by changing the ratio of oxidizer and fuel, it is possible to obtain cobalt oxide nanoparticles with specified properties and structure, which expands the scope of the product application.

Table 1. Methods of cobalt oxide synthesis

№	Method	Advantages	Disadvantages	Ref.
1	Thermal decomposition	1. Simple and inexpensive method 2. Cobalt oxide with high purity	1. High temperatures required 2. Complexity of particle size control	[25]
2	Sol-gel	1. Cobalt oxide with high dispersibility 2. Suitable for making thin films and coatings	1. It is a time-consuming process, and specialized equipment is required 2. Does not have the ability to economically scale	[26]
3	Spray pyrolysis	1. Can be used to create thin films and coatings 2. Process is highly controllable	1. The specialized equipment is required 2. The possibility of formation of irregular films	[27]
4	Hydrothermal method	1. Applicable to produce nanostructured materials	1. High pressure and temperature are required 2. The specialized equipment is required	[28]
5	Co-precipitation	1. Control of composition and structure 2. Formation of nanostructures 3. Reduction of temperature conditions	1. Complex tuning of experimental conditions and/or expensive reagents are required 2. Tendency of synthesis products to aggregate 3. Does not suitable for mass production	[29]

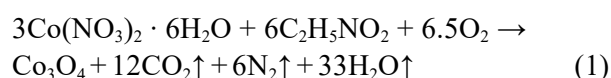
2. Experimental part

2.1. Materials

The following materials and equipment were used in this work: cobalt nitrate hexahydrate ($\text{Co}(\text{NO}_3)_2 \cdot 6\text{H}_2\text{O}$), glycine ($\text{C}_2\text{H}_5\text{NO}_2$) and nitric acid (all reagents were chemically or analytically grade); magnetic stirrer (MS-H340-S4); and laboratory plate.

2.2. Synthesis of Co_3O_4 by solution combustion method

The synthesis of ultra-disperse metal oxide particles is based on the exothermic process of interaction between the components of the solution system: fuel and oxidizer. Co_3O_4 nanoparticles were synthesized by the solution combustion method. Cobalt nitrate hexahydrate ($\text{Co}(\text{NO}_3)_2 \cdot 6\text{H}_2\text{O}$) as oxidizer and glycine ($\text{C}_2\text{H}_5\text{NO}_2$) as fuel were used to produce cobalt oxide. The reaction equation of glycine-nitrate synthesis of cobalt oxide is as follows:



The influence of the ratio of fuel and oxidizer on the morphology of the obtained nanoparticles was investigated. For this purpose, synthesis was carried out from a mixture of cobalt nitrate hexahydrate and glycine in the stoichiometric ratio $\varphi=1$ (3 moles of cobalt nitrate to 6 moles of glycine) and under the condition of a fuel-rich mixture $\varphi=1.5$ (for 3 moles of cobalt nitrate – 9 moles of glycine). The effect of nitric acid addition on the dispersion of cobalt oxide was investigated. Nitric acid was added in an amount of 10% by weight of cobalt nitrate.

The initial reagents were completely dissolved in 50 ml distilled water in a heat-resistant beaker and then evaporated to a volume of 5–7 ml. After evaporation, the reaction mixture was heated to 260 °C, whereupon spontaneous ignition of the solution was observed. The decomposition temperature of glycine was taken into account while selecting the self-ignition temperature. The ignition of the fuel mixture in solution leads to a temperature increase to 1200 °C and precipitation of the final product. The product of synthesis was washed with distilled water, and then dried at 80 °C for 24 h.

2.3. Methods of Co_3O_4 characterization

Currently, microscopic techniques are widely used to analyze the structure of various materials, including nanoparticles, and have an essential role for their characterization. These techniques include visible spectrum imaging, scanning electron microscopy (SEM) and transmission electron microscopy (TEM). One of the significant advantages of visual methods is the ability to represent structure in different regions of the samples. Thus, the images obtained provide information useful for comparing localized structures throughout the sample. Despite these advantages, optical methods do not provide the quantitative data necessary for comparative analysis of different nanoparticles. Therefore, samples were examined by energy-dispersive X-ray spectroscopy (EDX) to determine the elemental composition.

2.3.1. Transmission electron microscopy

Transmission electron microscope (TEM) JEM-1011 in the Kazakhstan-Japan Innovation Center of the Kazakh National Agrarian University from JEOL company from Japan was used to study the structure of cobalt oxide. This microscope is equipped with a Morada digital camera (Olympus, Japan). Its main specifications include an accelerating voltage that can be adjusted from 40 to 100 kV, an accurate resolution of 0.3 nm, a linear resolution of 0.14 nm, a LaB6 electron gun, and a magnification range from 100 to 1,000,000. This technique plays an important role in the development and characterization of various nanomaterials, including nanoparticles, and is an integral part of modern nanotechnology and materials science.

2.3.2. Scanning electron microscopy

Quanta 200i 3D scanning electron microscope (FEI, USA) with an accelerating voltage of 30 kV was used to study the structure, size, and morphology of samples ("National Nanotechnology Laboratory of Open Type" Al-Farabi KazNU, Almaty, Kazakhstan). This method allows imaging of the surface, which makes it possible to determine both the structure and size of individual particles. This microscope also has an energy-dispersive X-ray analysis (EDX) system that can determine the chemical composition in the B to U range, with a resolution of 132 eV ($\text{Mn K}\alpha$). EDX analysis was used to determine the chemical

composition of cobalt oxide nanoparticles and quantitative data.

2.3.3. X-ray diffraction analysis

The crystal structure of the nanomaterial samples was investigated through X-ray diffraction analysis (XRD) using a DRON-3M multipurpose X-ray diffractometer with copper radiation, which has an IBMPC-based control and recording system in digital form. XRD was used to obtain data on the lattice parameters of the substances, to determine their phase composition and the degree of amorphousness of the sample. The samples were examined under the following imaging settings: the X-ray tube voltage reached 30 kV, the tube current was 30 mA, and the goniometer was moved with an angular step of 0.05° 2θ while measuring the intensity up to 1.0. The sample was rotated in its plane at a speed of 60 rpm. Analysis of the X-ray data to determine the angle and intensity of reflection was performed using the program "Fpeak". Phase analysis was performed using the program "PCPDFWIN" and the diffraction data database. The obtained spectra were identified using the JCPDS X-ray database. The apparatus error of X-ray pulse measurement was less than 0.4%.

2.3.4 Small-angle X-ray scattering method

To investigate the nanoscale catalyst particles, small-angle X-ray scattering was applied. SAXS curves were analyzed using a Hecus S3-MICRO diffractometer with a Cu-C radiation filter. The value of the scattering vector modulus $q=4\cdot\pi\cdot\sin\Theta/\lambda$, where 2Θ is the scattering angle, λ is the wavelength of the

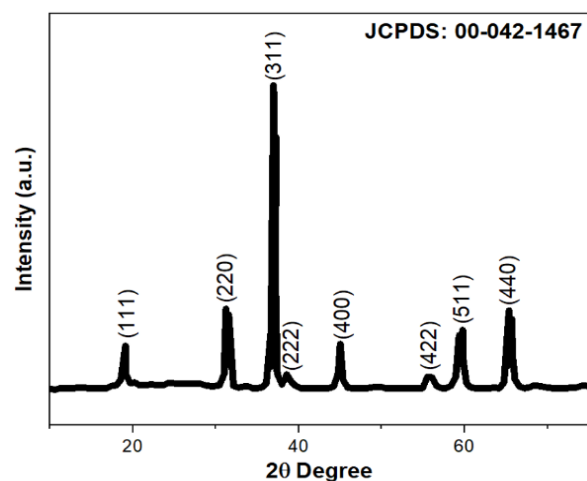


Fig. 1. Diffractogram of cobalt oxide obtained by solution combustion method of cobalt glycine-nitrate mixture at $\varphi=1.5$.

radiation used, thus λ was equal to 1.54 Å and 2Θ was equal to $0.008\div 8$) was used as the scattering coordinate. The scattering intensity was recorded in the range q from 0.006 to 0.6 \AA^{-1} ; q is linearly related to the correlation $L\sim 2\pi/q$. The small-angle curves for glycerol and several samples of nanoparticles dissolved in glycerol and obtained by the SAXS method were used to determine the size distribution (radius histogram) in the spherical approximation for nanoparticles.

3. Results and discussion

To establish the chemical and phase composition of the synthesized cobalt oxide nanoparticles, X-ray diffraction analysis was carried out, which showed that in all cases monophasic cobalt oxide with the formula Co_3O_4 was obtained (Fig. 1).

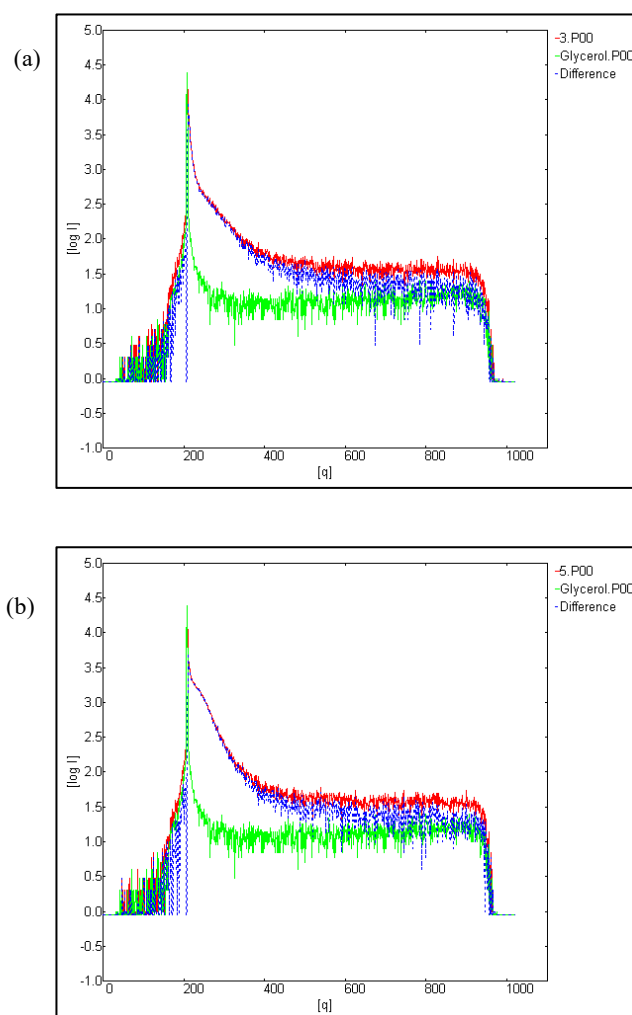


Fig. 2. Small-angle curves of glycerol and Co_3O_4 nanoparticles ($\varphi=1$): (a) Co_3O_4 nanoparticles obtained without addition of nitric acid ($\varphi=1$); (b) Co_3O_4 nanoparticles obtained with addition of nitric acid ($\varphi=1$).

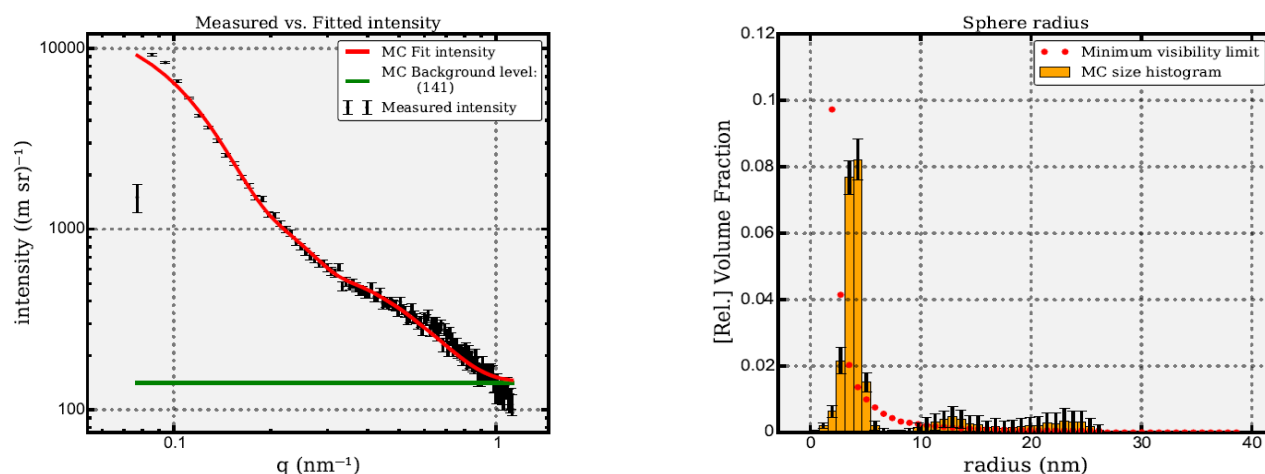


Fig. 3. Size distribution of Co_3O_4 nanoparticles in spherical approximation without addition of nitric acid ($\varphi=1$).

The diffractogram shows a characteristic diffraction pattern with a series of distinct peaks corresponding to planes (111), (220), (311), (222), (400), (511) and (440). The diffraction peaks and reflections are consistent with JCPDS card: 00-042-1467 [31]. All reflections are attributed to the typical Co_3O_4 phase. The monophasic cobalt oxide Co_3O_4 has a crystal symmetry corresponding to the crystal structure of spinel. The spinel structure is a type of cubic crystal structure with a space group known as $\text{Fd}3\text{m}$ (face-centered cubic structure), which is also referred to as a "cubic densely packed" structure. In the spinel structure, Co_3O_4 consists of two different types of cations (Co^{2+} and Co^{3+} cobalt ions) distributed in a specific order within the crystal lattice. This arrangement results in the characteristic symmetry of the $\text{Fd}3\text{m}$ spinel structure. In the Co_3O_4 spinel structure, oxygen ions (O^{2-}) form a tightly packed face-centered cubic (FCC) lattice, while cobalt ions

occupy both octahedral and tetrahedral positions within this oxygen lattice. The arrangement of cobalt ions within these positions contributes to the unique symmetry of Co_3O_4 as a spinel. To establish the chemical and phase composition of the synthesized cobalt oxide nanoparticles, X-ray diffraction analysis was carried out, which showed that in all cases monophasic cobalt oxide with the formula Co_3O_4 was obtained (Fig. 1).

To determine the effect of nitric acid, experiments were carried out without and with the addition of nitric acid to the initial mixture. The obtained samples were investigated by small-angle X-ray scattering. Glycerol was used as a matrix. Small-angle curves for glycerol and Co_3O_4 nanoparticles ($\varphi=1$, without the addition of nitric acid) and Co_3O_4 ($\varphi=1$, with the addition of nitric acid) (Fig. 2a, 2b). The contribution of small-angle scattering of glycerol was subtracted from the curve to determine the size distribution of

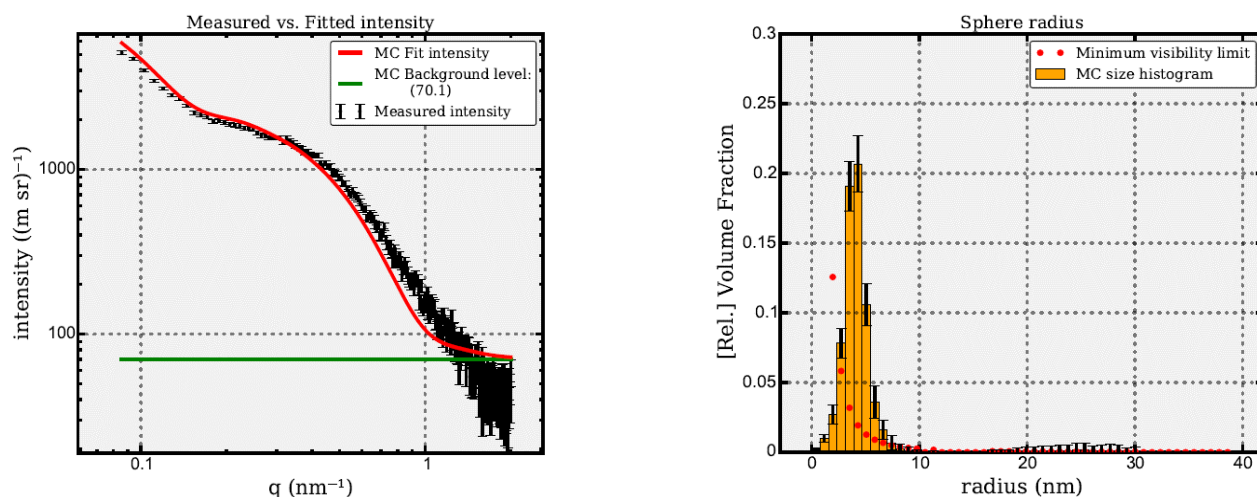


Fig. 4. Size distribution of Co_3O_4 nanoparticles in the spherical approximation with the addition of nitric acid ($\varphi=1$).

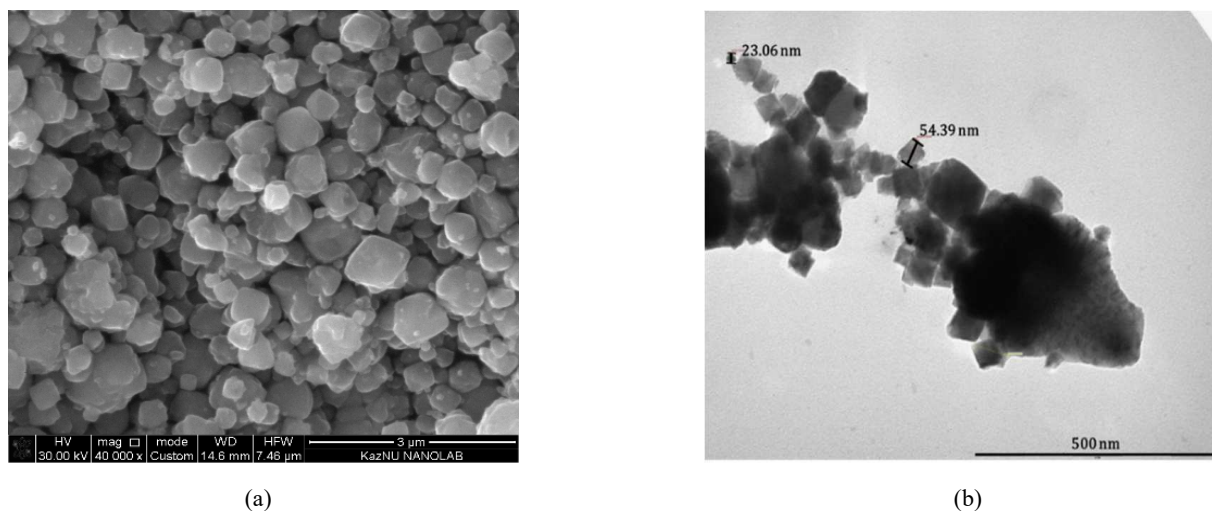


Fig. 5. Microscopic images of Co_3O_4 nanoparticles at $\phi=1$ with the addition of nitric acid: (a) SEM image: (b) TEM image.

nanoparticles (the sphere radius is indicated in the histogram) in the spherical approximation.

As can be seen from the graph of the distribution of cobalt oxide nanoparticles by diameter, 8% of particles have a diameter close to 5 nm, about 9–10% of nanoparticles have diameters up to 4 nm, a diameter of 5–6 nm corresponds to 1.5% of the studied nanoparticles, the contribution of the remaining nanoparticles is less 1%. The remaining fraction of nanoparticles has dimensions much larger than the maximum permissible diameter, so their contribution is not taken into account and is not displayed on the graph.

As can be seen from the distribution plot of Co_3O_4 nanoparticles obtained without the addition of nitric acid (Fig. 3), the main fraction of particles has a diameter up to 6 nm, but particles with diameters up to 25 nm are also present.

As can be seen from the distribution graph of Co_3O_4 nanoparticles obtained with the addition of nitric acid (Fig. 4), the bulk of the particles have diameters up to 8 nm. In this case, the nanoparticles have diameters up to 10 nm and there are no particles with larger diameters. The results obtained showed that the addition of nitric acid allows obtaining more monodisperse particles with a small spread.

As can be seen from the obtained scanning and transmission electron microscope images (Fig. 5), for cobalt oxide particles at stoichiometric fuel-to-oxidizer ratio $\phi=1$, the particle size range is from 23 to 60 nm, and agglomerates larger than 500 nm are also present. The formation of agglomerates can be attributed to high-temperature fluctuations during the self-ignition of the mixture. For the cobalt oxide nanoparticles at a ratio of $\phi=1.5$, the particle size ranges from 20 to 65 nm, without large agglomerates

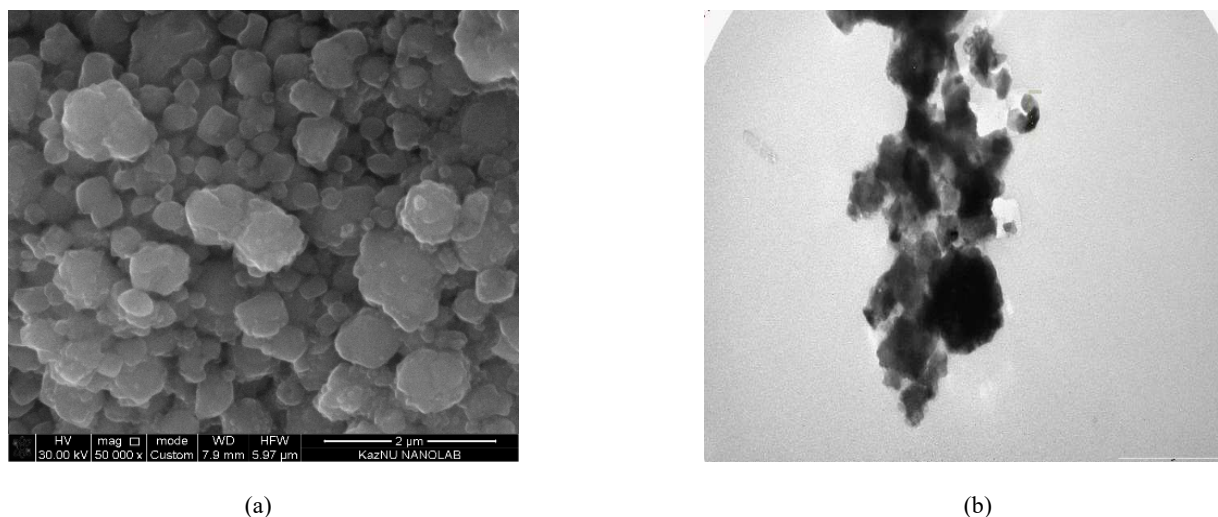


Fig. 6. Microscopic images of Co_3O_4 nanoparticles at $\phi=1.5$ with the addition of nitric acid: (a) SEM image: (b) TEM image.

Table 2. Key parameters of Co_3O_4 – based gas sensors

Electrode material composition	Sensitivity	Gas concentration (ppm)	Operating temperature ($^{\circ}\text{C}$)	Detected gas	Ref.
Co_3O_4	12	100	175	Ethanol	[35]
Co_3O_4	11.2	100	160	NH_3	[36]
Co_3O_4	11.4	100	150	Acetone	[37]
Co_3O_4	~14	100	160	Ethanol	[38]
Co_3O_4	5.4	10	300	Ethanol	[39]
Co_3O_4	5	100	160	Acetone	[40]
$\text{Co}_3\text{O}_4/\text{SnO}_2$	13.6	100	200	NH_3	[41]
$\text{Co}_3\text{O}_4/\text{WO}_3$	6.1	2000	200	H_2	[42]
$\text{Co}_3\text{O}_4/\text{ZnO}$	30	100	20	NO_2	[43]
$\text{Co}_3\text{O}_4/\text{TiO}_2$	16	100	140	CO	[44]
$\text{Co}_3\text{O}_4/\text{Ag}$	~5	5-1500	50-200	CO	[45]
$\text{Co}_3\text{O}_4/\text{CuO}$	1.5	100	160	NO_2	[46]

(Fig. 6). A comparison of the two samples based on SEM and TEM images illustrates the positive effect of fuel addition above the stoichiometric ratio. The reaction of the fuel with the oxidizer leads to the decomposition of the initial components with the formation of gaseous products that lead to further dispersion of the final product.

Thus, the obtained results confirm the efficiency of the synthesis of Co_3O_4 nanoparticles by the solution combustion method. Changing the composition of the initial mixture can significantly change the morphology of the obtained product and clearly illustrates the possibility of controlled synthesis. The synthesized Co_3O_4 nanoparticles are perspective materials for application in gas sensors.

Co_3O_4 as a transition metal oxide has chemical, phase, and structural stability, which allows increasing the temperature if necessary, and high electrical conductivity, which allows recording the chemoresistive response that occurs during the redox reactions of metal oxide with the detected gas [2, 32]. For this purpose, in metal-oxide gas sensors, the sensitive material Co_3O_4 is heated at a certain temperature. The flow of electricity within this material depends on the number of free electrons. When the sensing material is in clean air, the oxygen (O_2) in the atmosphere adsorbs on the surface of the sensing material, attracts free electrons, and keeps the electrons on the surface as ions. This leads to an increase in the resistance of the sensor, resulting in a

decrease in the flow of electrons within the sensing material. In the presence of reducing gases such as methane or propane, these gases interact with the adsorbed oxygen, releasing bound electrons within the sensing material. This results in a decrease in the resistance of the sensor, allowing more electrical current to flow. As the concentration of reducing gases increases, the resistance of the sensor decreases further, allowing even more electrical current to flow. According to the sensitivity characteristics of Co_3O_4 , there is a certain relationship between the sensor resistance and the gas concentration in the atmosphere, which provides information about the concentration of pollutants in the air [33, 34].

In Table 2, examples of Co_3O_4 applications in gas sensors for the determination of a wide range of gases are shown. The main parameters of Co_3O_4 – based gas sensors are given.

Successful results of Co_3O_4 application in gas sensors show the prospect and relevance of the development and optimization of methods for obtaining cobalt oxide nanoparticles with controlled parameters of morphology and structure to obtain stable and repeatable results.

4. Conclusion

Co_3O_4 nanoparticles were obtained by solution combustion method as a result of the exothermic redox reaction of cobalt nitrate hexahydrate

($\text{Co}(\text{NO}_3)_2 \cdot 6\text{H}_2\text{O}$) and glycine ($\text{C}_2\text{H}_5\text{NO}_2$). The effect of the addition of nitric acid and the fuel: oxidizer ratio on the structure and dispersibility of cobalt oxide nanoparticles was investigated. The positive effect of the addition of nitric acid was established. The addition of nitric acid allows to obtain of cobalt oxide nanoparticles with a more uniform distribution of particles, which is proved by SAXS investigations. Moreover, it was found that the use of a fuel-rich mixture ($\varphi=1.5$) leads to the formation of more homogeneous Co_3O_4 crystals with a size of 23–60 nm. Thus, by changing the composition and ratio of components of the initial mixture it is possible to qualitatively change the structure and morphology of the final product. Co_3O_4 nanoparticles obtained by solution combustion method is a potential and perspective sensitive material for gas sensors, while manipulation of the synthesis process allows to obtain nanoparticles with a given structure and properties. Thus, it allows Co_3O_4 nanoparticles-based gas sensors to be used further in the military, metallurgy, and oil-producing industries, which expands the scope of potential application of cobalt oxide nanoparticles obtained by solution combustion method.

Acknowledgment

This work was funded by the Ministry of Science and Higher Education of the Republic of Kazakhstan (Grant AP19679885).

References

- [1]. Giovanni N. First Fifty Years of Chemoresistive Gas Sensors // *Chemosensors*. – 2015 – Vol. 20
- [2]. Wang C., Yin L., Zhang L., Xiang D., Gao R. Metal oxide gas sensors: sensitivity and influencing factors // *sensors*. – 2010. – Vol. 10. – №. 3. – P. 2088-2106.
- [3]. Korotcenkov G. The role of morphology and crystallographic structure of metal oxides in response of conductometric-type gas sensors // *Materials Science and Engineering: R: Reports*. – 2008. – Vol. 61. – №. 1-6. – P. 1-39.
- [4]. Barsan N., Koziej D., Weimar U. Metal oxide-based gas sensor research: How to? // *Sensors and Actuators B: Chemical*. – 2007. – Vol. 121. – №. 1. – P. 18-35.
- [5]. Chatterjee S.G., Chatterjee S., Ray A.K., Chakraborty A.K. Graphene-metal oxide nanohybrids for toxic gas sensor: A review // *Sensors and Actuators B: Chemical*. – 2015. – Vol. 221. – P. 1170-1181.
- [6]. Liu H., Zhang L., Li K.H.H., Tan O. K. Microhotplates for metal oxide semiconductor gas sensor applications – Towards the CMOS-MEMS monolithic approach // *Micromachines*. – 2018. – Vol. 9. – №. 11. – P. 557.
- [7]. Fine G.F., Cavanagh L.M., Afonja A., Binions R. Metal oxide semi-conductor gas sensors in environmental monitoring // *sensors*. – 2010. – Vol. 10. – №. 6. – P. 5469-5502.
- [8]. Saritas S., Kundakci M., Coban O., Tuzemen S., Yildirim M. Ni: Fe_2O_3 , Mg: Fe_2O_3 and Fe_2O_3 thin films gas sensor application // *Physica B: Condensed Matter*. – 2018. – Vol. 541. – P. 14-18.
- [9]. Choi S., Bonyani M., Sun G. J., Lee J. K., Hyun S. K., Lee C. Cr_2O_3 nanoparticle-functionalized WO_3 nanorods for ethanol gas sensors // *Applied Surface Science*. – 2018. – Vol. 432. – P. 241-249.
- [10]. Wang C., Cui X., Liu J., Zhou X., Cheng X., Sun P., Hu X., Li X., Zheng J., Lu G. Design of superior ethanol gas sensor based on Al-doped NiO nanorod-flowers // *ACS Sensors*. – 2016. – Vol. 1. – №. 2. – P. 131-136.
- [11]. Zhu L., Zeng W. Room-temperature gas sensing of ZnO-based gas sensor: A review // *Sensors and Actuators A: Physical*. – 2017. – Vol. 267. – P. 242-261.
- [12]. Kondalkar V.V., Duy L.T., Seo H., Lee K. Nanohybrids of Pt-functionalized $\text{Al}_2\text{O}_3/\text{ZnO}$ core-shell nanorods for high-performance MEMS-based acetylene gas sensor // *ACS applied materials & interfaces*. – 2019. – Vol. 11. – №. 29. – P. 25891-25900.
- [13]. Das S., Jayaraman V. SnO_2 : A comprehensive review on structures and gas sensors // *Progress in Materials Science*. – 2014. – Vol. 66. – P. 112-255.
- [14]. Nisar J., Topalian Z., De Sarkar A., Österlund L., Ahuja R. TiO_2 -based gas sensor: a possible application to SO_2 // *ACS applied materials & interfaces*. – 2013. – Vol. 5. – №. 17. – P. 8516-8522.
- [15]. Dong C., Zhao R., Yao L., Ran Y., Zhang X., Wang Y. A review on WO_3 based gas sensors: Morphology control and enhanced sensing properties // *Journal of Alloys and Compounds*. – 2020. – Vol. 820. – P. 153194.
- [16]. Haiduk Y.S., Savitsky A.A., Khort A.A. WO_3 - Co_3O_4 Compositions Prepared by the Sol-Gel Process: Structure and Gas-Sensing Properties // *Russian Journal of Inorganic Chemistry*. – 2019. – Vol. 64. – P. 717-724.

- [17]. Vojisavljević K., Wicker S., Can I., Benčan A., Barsan N., Malič B. Nanocrystalline cobalt-oxide powders by solution-combustion synthesis and their application in chemical sensors // *Advanced Powder Technology*. – 2017. – Vol. 28. – №. 4. – P. 1118-1128.
- [18]. Deng J., Kang L., Bai G., Li Y., Li P., Liu X., Liang W. Solution combustion synthesis of cobalt oxides (Co_3O_4 and $\text{Co}_3\text{O}_4/\text{CoO}$) nanoparticles as supercapacitor electrode materials // *Electrochimica Acta*. – 2014. – Vol. 132. – P. 127-135.
- [19]. Liu Y., Zhang X. Effect of calcination temperature on the morphology and electrochemical properties of Co_3O_4 for lithium-ion battery // *Electrochimica Acta*. – 2009. – Vol. 54. – №. 17. – P. 4180-4185.
- [20]. Acedera R.A.E., Gupta G., Mamlouk M., Balela M.D.L. Solution combustion synthesis of porous Co_3O_4 nanoparticles as oxygen evolution reaction (OER) electrocatalysts in alkaline medium // *Journal of Alloys and Compounds*. – 2020. – Vol. 836. – P. 154919.
- [21]. Toniolo J.C., Takimi A.S., Bergmann C.P. Nanostructured cobalt oxides (Co_3O_4 and CoO) and metallic Co powders synthesized by the solution combustion method // *Materials Research Bulletin*. – 2010. – Vol. 45. – №. 6. – P. 672-676.
- [22]. Filatova N.Vol., Býshkova T.M., Kosenko N.F., Býgrova Iý. S. Difraktoметрическое исследование синтеза кобальтсодержащего керамического пигмента из оксидных прекурсоров (Diffraction study of synthesis of cobalt-containing ceramic pigment from oxide precursors) // *Научный взгляд в будущее* (Scientific insight into the future) – 2018. – Vol. 3. – №. 11. – P. 112-118.
- [23]. Kozlovskiy A.L., Zdorovets M.V. The study of the structural characteristics and catalytic activity of $\text{Co}/\text{CoCo}_2\text{O}_4$ nanowires // *Composites Part B: Engineering*. – 2020. – Vol. 191. – P. 107968.
- [24]. Chaudhary A., Pathak D. K., Ghosh T., Kandpal S., Tanwar M., Rani C., Kumar R. Prussian blue-cobalt oxide double layer for efficient all-inorganic multicolor electrochromic device // *ACS Applied Electronic Materials*. – 2020. – Vol. 2. – №. 6. – P. 1768-1773.
- [25]. Liu X., Yi R., Zhang N., Shi R., Li X., Qiu G. Cobalt hydroxide nanosheets and their thermal decomposition to cobalt oxide nanorings // *Chemistry-An Asian Journal*. – 2008. – Vol. 3. – №. 4. – P. 732-738.
- [26]. Farahmandjou M. Fabrication and characterization of nanoporous Co oxide (Co_3O_4) prepared by simple sol-gel synthesis // *Physical Chemistry Research*. – 2016. – Vol. 4. – №. 2. – P. 153-160.
- [27]. Moro F., Tang S. V.Y., Tuna F., Lester E. Magnetic properties of cobalt oxide nanoparticles synthesised by a continuous hydrothermal method // *Journal of magnetism and magnetic materials*. – 2013. – Vol. 348. – P. 1-7.
- [28]. Shinde V.R., Mahadik S.B., Gujar T.P., Lokhande, C. D. Supercapacitive cobalt oxide (Co_3O_4) thin films by spray pyrolysis // *Applied Surface Science*. – 2006. – Vol. 252. – №. 20. – P. 7487-7492.
- [29]. Thambidurai S., Gowthaman P., Venkatachalam M., Suresh S., Kandasamy M. Morphology dependent photovoltaic performance of zinc oxide-cobalt oxide nanoparticle/nanorod composites synthesized by simple chemical co-precipitation method // *Journal of Alloys and Compounds*. – 2021. – Vol. 852. – P. 156997.
- [30]. Sinkó K., Szabó G., Zrínyi M. Liquid-phase synthesis of cobalt oxide nanoparticles // *Journal of Nanoscience and Nanotechnology*. – 2011. – Vol. 11. – №. 5. – P. 4127-4135.
- [31]. Pudukudy M., Yaakob Z. Sol-gel synthesis, characterisation, and photocatalytic activity of porous spinel Co_3O_4 nanosheets // *Chemical Papers*. – 2014. – Vol. 68. – P. 1087-1096.
- [32]. Dey A. Semiconductor metal oxide gas sensors: A review // *Materials science and Engineering: B*. – 2018. – Vol. 229. – P. 206-217.
- [33]. Patil S.J., Patil A.V., Dighavkar C.G., Thakare K.S., Borase R.Y., Nandre S.J., Deshpande N.G., Ahire R.R. Semiconductor metal oxide compounds based gas sensors: A literature review // *Frontiers of Materials Science*. – 2015. – Vol. 9. – P. 14-37.
- [34]. Simonenko N.P., Fisenko N.A., Fedorov F.S., Simonenko T.L., Mokrushin A.S., Simonenko E. P., Korotcenkov G., Sysoev V.V., Kuznetsov N.T. Printing technologies as an emerging approach in gas sensors: Survey of literature // *Sensors*. – 2022. – Vol. 22. – №. 9. – P. 3473.
- [35]. Bhalerao K.D., Khan M., Nakata Y.T., Kadam R. M., Mansoor S., Maserati S., Mishra P., Nakata U. T., Ahmad R. Co_3O_4 hexagonal nanodisks: Synthesis and efficient ethanol gas sensing application // *Surfaces and Interfaces*. – 2023. – P. 103350.
- [36]. Deng J., Zhang R., Wang L., Lou Z., Zhang T. Enhanced sensing performance of the Co_3O_4 hierarchical nanorods to NH_3 gas // *Sensors and Actuators B: Chemical*. – 2015. – Vol. 209. – P. 449-455.
- [37]. Zhang Z., Wen Z., Ye Z., Zhu L. Gas sensors based on ultrathin porous Co_3O_4 nanosheets to detect

- acetone at low temperature // RSC advances. – 2015. – Vol. 5. – №. 74. – P. 59976-59982.
- [38]. Wang X., Yao S., Wu X., Shi Z., Sun H., Que, R. High gas-sensor and supercapacitor performance of porous Co_3O_4 ultrathin nanosheets // RSC Advances. – 2015. – Vol. 5. – №. 23. – P. 17938-17944.
- [39]. Zhang P., Wang J., Lv X., Zhang H., Sun X. Facile synthesis of Cr-decorated hexagonal Co_3O_4 nanosheets for ultrasensitive ethanol detection // Nanotechnology. – 2015. – Vol. 26. – №. 27. – P. 275501.
- [40]. Lin Y., Ji H., Shen Z., Jia Q., Wang D. Enhanced acetone sensing properties of Co_3O_4 nanosheets with highly exposed (111) planes // Journal of Materials Science: Materials in Electronics. – 2016. – Vol. 27. – P. 2086-2095.
- [41]. Jeong H.M., Kim J.H., Jeong S.Y., Kwak C.H., Lee J.H. Co_3O_4 - SnO_2 hollow heteronanostructures: facile control of gas selectivity by compositional tuning of sensing materials via galvanic replacement // ACS Applied Materials & Interfaces. – 2016. – Vol. 8. – №. 12. – P. 7877-7883.
- [42]. Park S., Sun G.J., Kheel H., Hyun S.K., Jin C., Lee C. Hydrogen gas sensing of Co_3O_4 -Decorated WO_3 nanowires // Metals and Materials International. – 2016. – Vol. 22. – P. 156-162.
- [43]. Park S., Kim S., Kheel H., Lee C. Oxidizing gas sensing properties of the n-ZnO/p- Co_3O_4 composite nanoparticle network sensor // Sensors and Actuators B: Chemical. – 2016. – Vol. 222. – P. 1193-1200.
- [44]. Li S., Wei X., Zhu S., Zhou Q., Gui Y. Low temperature carbon monoxide gas sensor based on Co_3O_4 @ TiO_2 nanocomposites: theoretical and experimental analysis // Journal of Alloys and Compounds. – 2021. – Vol. 882. – P. 160710.
- [45]. Molavi R., Sheikhi M.H. Low temperature carbon monoxide gas sensor based on Ag- Co_3O_4 thick film nanocomposite // Materials Letters. – 2018. – Vol. 233. – P. 74-77.
- [46]. Fang H., Li S., Zhao H., Deng J., Wang D., Li J. Enhanced NO_2 gas sensing performance by hierarchical CuO - Co_3O_4 spheres // Sensors and Actuators B: Chemical. – 2022. – Vol. 352. – P. 131068.
- [2]. Wang C, Yin L, Zhang L, Xiang D, Gao R (2010) Sensors 10(3):2088-2106. <https://doi.org/10.3390/s100302088>
- [3]. Korotcenkov G (2008) Materials Science and Engineering: R: Reports. 61(1-6):1-39. <https://doi.org/10.1016/j.mser.2008.02.001>
- [4]. Barsan N, Koziej D, Weimar U (2007) Sensors and Actuators B: Chemical 121(1):18-35. <https://doi.org/10.1016/j.snb.2006.09.047>
- [5]. Chatterjee SG, Chatterjee S, Ray AK, Chakraborty AK (2015) Sensors and Actuators B: Chemical 221:1170-1181. <https://doi.org/10.1016/j.snb.2015.07.070>
- [6]. Liu H, Zhang L, Li KHH, Tan OK (2018) Micromachines 9(11):557. <https://doi.org/10.3390/mi9110557>
- [7]. Fine GF, Cavanagh LM, Afonja A, Binions R (2010) Sensors 10(6):5469-5502. <https://doi.org/10.3390/s100605469>
- [8]. Saritas S, Kundakci M, Coban O, Tuzemen S, Yildirim M (2018) Physica B: Condensed Matter 541:14-18. <https://doi.org/10.1016/j.physb.2018.04.028>
- [9]. Choi S, Bonyani M, Sun GJ, Lee JK, Hyun S K, Lee C (2018) Applied Surface Science 432:241-249. <https://doi.org/10.1016/j.apsusc.2017.01.245>
- [10]. Wang C, Cui X, Liu J, Zhou X, Cheng X, Sun P, Lu, G (2016) ACS Sensors 1(2):131-136. <https://doi.org/10.1021/acssensors.5b00123>
- [11]. Zhu L, Zeng W (2017) Sensors and Actuators A: Physical 267:242-261. <https://doi.org/10.1016/j.sna.2017.10.021>
- [12]. Kondalkar VV, Duy LT, Seo H, Lee K (2019) ACS applied materials & interfaces 11(29):25891-25900. <https://doi.org/10.1021/acscami.9b06338>
- [13]. Das S, Jayaraman V (2014) Progress in Materials Science 66:112-255. <https://doi.org/10.1016/j.pmatsci.2014.06.003>
- [14]. Nisar J, Topalian Z, De Sarkar A, Ö Sterlund L, Ahuja R. (2013) ACS applied materials & interfaces 5(17):8516-8522. <https://doi.org/10.1021/am4018835>
- [15]. Dong C, Zhao R, Yao L, Ran Y, Zhang X, Wang Y (2020) Journal of Alloys and Compounds 820:153194. <https://doi.org/10.1016/j.jallcom.2019.153194>
- [16]. Haiduk YS, Savitsky AA, Khort AA (2019) Russian Journal of Inorganic Chemistry 64:717-724. <https://doi.org/10.1134/S003602361906007X>
- [17]. Vojisavljević K, Wicker S, Can I, Benčan A, Barsan N, Malič B (2017) Advanced Powder Technology 28(4):1118-1128. <https://doi.org/10.1016/j.appt.2016.10.029>

References

- [1]. Neri G (2015) Chemosensors 3(1):1-20. <https://doi.org/10.3390/chemosensors3010001>

- [18]. Deng J, Kang L, Bai G, Li Y, Li P, Liu X, Liang W (2014) *Electrochimica Acta* 132:127-135. <http://dx.doi.org/10.1016/j.electacta.2014.03.158>
- [19]. Liu Y, Zhang X (2009) *Electrochimica Acta* 54(17):4180-4185. <https://doi.org/10.1016/j.electacta.2009.02.060>
- [20]. Acedera RAE, Gupta G, Mamlouk M, Balela MDL (2020) *Journal of Alloys and Compounds* 836:154919. <https://doi.org/10.1016/j.jallcom.2020.154919>
- [21]. Toniolo JC, Takimi AS, & Bergmann CP (2010) *Materials Research Bulletin* 45(6):672-676. <https://doi.org/10.1016/j.materresbull.2010.03.001>
- [22]. Filatova NV, Býshkova TM, Kosenko NF, BýgrovalýS (2018) *Scientific insight into the future [Naýchny vzglad v býdýee]* 3(11):112-118. <https://doi.org/10.30888/2415-7538.2018-11-03-026>
- [23]. Kozlovskiy AL, Zdorovets MV (2020) *Composites Part B: Engineering* 191:107968. <https://doi.org/10.1016/j.compositesb.2020.107968>
- [24]. Chaudhary A, Pathak DK, Ghosh T, Kandpal S, Tanwar M, Rani CK Kumar R (2020) *ACS Applied Electronic Materials* 2(6):1768-1773. <https://doi.org/10.1021/acsaelm.0c00342>
- [25]. Liu X, Yi R, Zhang N, Shi R, Li X, Qiu G (2008) *Chemistry-An Asian Journal* 3(4):732-738. <https://doi.org/10.1002/asia.200700264>
- [26]. Farahmandjou M (2016) *Physical Chemistry Research* 4(2):153-160. <https://doi.org/10.22036/pcr.2016.12909>
- [27]. Moro F, Tang SV Y, Tuna F, Lester E (2013) *Journal of magnetism and magnetic materials* 348:1-7. <https://doi.org/10.1016/j.jmmm.2013.07.064>
- [28]. Shinde VR, Mahadik SB, Gujar TP, Lokhande C D (2006) *Applied Surface Science* 252(20):7487-7492. <https://doi.org/10.1016/j.apsusc.2005.09.004>
- [29]. Thambidurai S, Gowthaman P, Venkatachalam M, Suresh S, Kandasamy M (2021) *Journal of Alloys and Compounds* 852:156997. <https://doi.org/10.1016/j.jallcom.2020.156997>
- [30]. Sinkó K, Szabó G, Zrínyi M (2011) *Journal of Nanoscience and Nanotechnology* 11(5):4127-4135. <https://doi.org/10.1166/jnn.2011.3875>
- [31]. Pudukudy M, Yaakob Z (2014) *Chemical Papers* 68:1087-1096. <https://doi.org/10.30799/jnst.S01.19050308>
- [32]. Dey A (2018) *Materials science and Engineering: B* 229:206-217. <https://doi.org/10.1016/j.mseb.2017.12.036>
- [33]. Patil SJ, Patil AV, Dighavkar CG, Thakare KS, Borase RY, Nandre SJ, Ahire RR (2015) *Frontiers of Materials Science* 9:14-37. <https://doi.org/10.1007/s11706-015-0279-7>
- [34]. Simonenko NP, Fisenko NA, Fedorov FS, Simonenko TL, Mokrushin AS, Simonenko EP, Kuznetsov NT (2022) *Sensors* 22(9):3473. <https://doi.org/10.3390/s22093473>
- [35]. Bhalerao KD, Khan M, Nakate YT, Kadam RM, Manzoor S, Masrat S, Ahmad R (2023) *Surfaces and Interfaces* 42:103350. <https://doi.org/10.1016/j.surfin.2023.103350>
- [36]. Deng J, Zhang R, Wang L, Lou Z, Zhang T (2015) *Sensors and Actuators B: Chemical* 209: 449-455. <https://doi.org/10.1016/j.snb.2014.11.141>
- [37]. Zhang Z, Wen Z, Ye Z, Zhu L (2015) *RSC advances* 5(74):59976-59982. <https://doi.org/10.1039/C5RA08536E>
- [38]. Wang X, Yao S, Wu X, Shi Z, Sun H, & Que, R. (2015) *RSC Advances* 5(23):17938-17944. <https://doi.org/10.1039/C4RA14450C>
- [39]. Zhang P, Wang J, Lv X, Zhang H, Sun X (2015) *Nanotechnology* 26(27):275501. <https://doi.org/10.1088/0957-4484/26/27/275501>
- [40]. Lin Y, Ji H, Shen Z, Jia Q, Wang D (2016) *Journal of Materials Science: Materials in Electronics* 27:2086-2095. <https://doi.org/10.1007/s10854-015-3995-y>
- [41]. Jeong HM, Kim JH, Jeong SY, Kwak CH, Lee JH (2016) *ACS Applied Materials & Interfaces* 8(12):7877-7883. <https://doi.org/10.1021/acsaami.6b00216>
- [42]. Park S, Sun GJ, Kheel H, Hyun SK, Jin C, Lee, C (2016) *Metals and Materials International* 22:156-162. <https://doi.org/10.1007/s12540-015-5376-8>
- [43]. Park S, Kim S, Kheel H, Lee C (2016) *Sensors and Actuators B: Chemical* 222:1193-1200. <https://doi.org/10.1016/j.snb.2015.08.006>
- [44]. Li S, Wei X, Zhu S, Zhou Q, Gui Y (2021) *Journal of Alloys and Compounds* 882:160710. <https://doi.org/10.1016/j.jallcom.2021.160710>
- [45]. Molavi R, Sheikhi MH (2018) *Materials Letters* 233:74-77. <https://doi.org/10.1016/j.matlet.2018.08.087>
- [46]. Fang H, Li S, Zhao H, Deng J, Wang D, Li J (2022) *Sensors and Actuators B: Chemical* 352:131068. <https://doi.org/10.1016/j.snb.2021.131068>

Сұйық фазалы жану әдісімен алынған Co_3O_4 нанобөлшектерінің морфологиялық ерекшеліктері

А. Кенешбекова^{1*}, А.Имаш^{1,2}, Б. Қайдар¹,
Э. Енсеп², А. Ильянов², М. Артыкбаева¹,
Н. Приходько^{1,3}, Г. Смагулова¹

¹Жану проблемалары институты, Бөгенбай батыр к., 172, Алматы, Қазақстан

²Әл-Фараби атындағы Қазақ ұлттық университеті, әл-Фараби даң., 71, Алматы, Қазақстан

³Ғұмарбек Дәукеев атындағы Алматы энергетика және байланыс университеті, Байтұрсынұлы к. 126/1, Алматы, Қазақстан

АННОТАЦИЯ

Жаһандық экологиялық дағдарыс қоршаған орта параметрлерін бақылау және талдау құралдары мен әдістерін жетілдіруді қажет етті. Ауа сапасын бағалау үшін өте маңызды газ датчиктері зиянды заттарды анықтаудың дәлдігі мен тиімділігін арттыру мақсатында үнемі жетілдіріліп отырады. Олар жұмыс орындарында, қалалық жерлерде және өнеркәсіптік нысандарда қауіпсіздікті қамтамасыз етуде маңызды рөл атқарады, бұл ластанумен күресуге көмектеседі. Газ датчиктерінің жақсартылған өнімділігі газға сезімтал материалдарды және олардың құрылымын мұқият таңдау мен бақылауға байланысты. Бұған газға сезімтал қосылыстарды оңтайландыру, озық материалдарды пайдалану және заттарды сезімтал және жылдам анықтау технологияларын әзірлеу кіреді.

Осы мақсат үшін перспективалы қосылыстардың бірі – сұйық-фазалық жану әдісімен тиімді синтезделген Co_3O_4 оксиді. Бұл әдіс қарапайымдылығымен ерекшеленеді және өнімнің құрылымы мен қасиеттерін дәл бақылауға, оны нақты талаптарға бейімдеуге мүмкіндік береді және анықтаудың жоғары тиімділігі мен дәлдігін қамтамасыз етеді. Бұл зерттеуде Co_3O_4 бөлшектері сұйық-фазалық жану әдісі арқылы азот қышқылы қосылған кобальт нитраты мен глицин қоспасынан синтезделді. Кобальт оксидінің морфологиялық сипаттамаларына азот қышқылының қосылуы мен отын-тотықтырғыш қатынасының әсері зерттелді. SEM, TEM, XRD және SAXS талдауларының нәтижелері азот қышқылы мен отынмен байытылған қоспаның қосылуы диаме-

трі кішірек дисперсия және тұрақты қасиеттері бар нанобөлшектерге әкелетінін растады.

Кілт сөздер: металл-оксидті наноматериалдар, Co_3O_4 нанобөлшектері, сұйық фазалық жану әдісі, экзотермиялық тотығу-тотықсыздану реакциясы, газ датчиктері.

Морфологические особенности наночастиц Co_3O_4 полученных методом жидкофазного горения

А. Кенешбекова^{1*}, А. Имаш^{1,2}, Б. Кайдар¹,
Э. Енсеп², А. Ильянов², М. Артыкбаева¹,
Н. Приходько^{1,3}, Г. Смагулова¹

¹Институт проблем горения, ул. Бөгенбай батыра 172, Алматы, Казахстан

²Казахский национальный университет им. аль-Фараби, пр. аль-Фараби 71, Алматы, Казахстан

³Алматинский университет энергетике и связи им. Г. Даукеева, ул. Байтұрсынұлы 161/1, Алматы, Казахстан

АННОТАЦИЯ

В связи с глобальным экологическим кризисом возникает необходимость совершенствования средств и методов мониторинга и анализа параметров окружающей среды. Газовые датчики, играющие важнейшую роль в оценке качества воздуха, постоянно совершенствуются с целью повышения точности и эффективности обнаружения вредных веществ. Они играют важную роль в обеспечении безопасности на рабочих местах, в городах и промышленных объектах, способствуя борьбе с загрязнением окружающей среды. Повышение эффективности газовых сенсоров зависит от тщательного подбора и контроля газочувствительных материалов и их структуры. Для этого необходимо оптимизировать газочувствительные соединения, использовать современные материалы и разрабатывать технологии для чувствительного и быстрого обнаружения веществ. Одним из перспективных соединений для этих целей является оксид Co_3O_4 , эффективно синтезированный методом жидкофазного горения. Этот метод отличается простотой и позволяет точно контролировать структуру и свойства продукта, что дает возможность адаптировать его к конкретным требованиям и обеспечить высокую эффективность и точность обнаружения. В дан-

ной работе частицы Co_3O_4 были синтезированы из смеси нитрата кобальта и глицина с добавлением азотной кислоты методом жидкофазного горения. Было исследовано влияние добавления азотной кислоты и соотношение горючего к окислителю на морфологические характеристики получаемого оксида кобальта. Результаты СЭМ, ПЭМ, РФА и МУРР анализов подтверждают, что добавление

азотной кислоты и использование топливо-богатой смеси приводят к образованию наночастиц с меньшим разбросом по диаметру и более стабильными показателями.

Ключевые слова: металл-оксидные наноматериалы, наночастицы Co_3O_4 , метод жидкофазного горения, экзотермическая окислительно-восстановительная реакция, газовые сенсоры.